



# MODELAIR – DELIVERABLE

## D3.3 – EXPERIMENTAL DATABASES (VELOCITY FIELDS)

This report is part of a project that has received funding from the European Union's Horizon Europe MSCA Doctoral Networks 2021 programme under **Grant Agreement No. 101072559**

**Deliverable number:** D3.3

**Due date:** 31<sup>st</sup> December 2024

**Type<sup>1</sup>:** O

**Dissemination Level<sup>1</sup>:** PU

**Work Package:** WP3

**Lead Beneficiary:** University of Bristol (UoB)

**Contributing Beneficiaries:** MT

---

1

**Type** R = Report ADM = Administrative PDE = diss./ex. O = Other  
DEC = Websites, patents filing, press & media actions, videos, etc.

**Dissemination Level** PU = Public  
CO = Confidential, only for members of the consortium (including the Commission Services)  
CI = Classified  
SEN = Sensitive, limited under the conditions of the Grant Agreement

## DOCUMENT HISTORY



**Deliverable leader:** Nada Taouil, Mahdi Azarpeyvand.

**E-mail of lead author:** [vv23404@bristol.ac.uk](mailto:vv23404@bristol.ac.uk)

**Reviewer(s):** Dani Fernández

Version	Date	Description
0.1	13/12/2024	Draft
0.2	18/12/2024	Reviewed
1.0	18/12/2024	<b><u>Final version</u></b>

### Abstract

This study investigates the characteristics of an artificially generated Atmospheric Boundary Layer (ABL) to validate its conformity with the standards for use in urban flow experiments. The ABL was created using a Counihan method [1] within the Boundary Layer Wind Tunnel (BLWT) at the University of Bristol, incorporating roughness elements, vortex generators, and castellated barriers to replicate urban turbulence conditions. Hot-wire measurements around a scaled model of Bristol city captured the flow dynamics, revealing the influence of building canopy and topographical variations on the ABL. The results demonstrate adherence to key turbulence metrics, including Kolmogorov's  $-5/3$  law, and provide critical insights into urban aerodynamic phenomena. Future work will employ advanced measurement techniques; including a 3D traverse system for hot-wire anemometry and Flame Ionisation Detector (FID) analysis, as well as Particle Image Velocimetry (PIV) for detailed flow visualisation and validation of computational models.

### Keywords

Atmospheric boundary layer, scaled model, hot-wire measurements, and urban flow.

### Acronyms

**ABL:** Atmospheric Boundary Layer

**AP:** Associated partner

**BEN:** Beneficiary

**BL:** Boundary Layer

## DOCUMENT HISTORY



**BLWT:** Boundary Layer Wind Tunnel

**CFD:** Computational Fluid Dynamics

**COO:** Coordinator

**CTA:** Constant Temperature Anemometry

**DEFRA:** Department for Environment, Food & Rural Affairs

**ESDU:** Engineering Sciences Data Unit

**FID:** Flame Ionisation Detector

**PIV:** Particle Image Velocimetry

### List of Participants

1	COO	Universidad Politécnica de Madrid	UPM	ES
2	BEN	BARCELONA SUPERCOMPUTING CENTER-CENTRO NACIONAL DE SUPERCOMPUTACION	BSC	ES
3	BEN	UNIVERSITE LIBRE DE BRUXELLES	ULB	BE
4	BEN	KUNGLIGA TEKNISKA HOEGSKOLAN	KTH	SE
5	BEN	OVE ARUP & PARTNERS SA	ARUP	ES
6	BEN	MICROFLOWN TECHNOLOGIES BV	MT	NL
7	AP	BuildWind SPRL	BW	BE
8	AP	BRISTOL CITY COUNCIL	BRIS CC	UK
9	AP	AYUNTAMIENTO DE MADRID	AY MAD	ES
10	AP	UNIVERSITY OF BRISTOL	UoB	UK
11	AP	AIR QUALITY CONSULTANTS LTD	AQC	UK



**Table of Contents**

1. Introduction .....5

2. Atmospheric boundary layer generation .....5

    2.1. Experimental set-up ..... 5

    2.2. Results and discussion..... 7

3. Bristol city wind tunnel model.....9

    3.1. Experimental set-up ..... 9

    3.2. Results and discussion..... 12

        3.2.1. City inflow conditions: smoothing ramp analysis ..... 12

        3.2.2. Flow throughout the city model ..... 14

4. Conclusions and future work.....19

References .....20

## 1. Introduction

Understanding flow dynamics in urban areas is critical for addressing challenges such as pollution dispersion, wind energy optimisation, and structural safety. Accurate simulation of these flows requires the generation of an (Atmospheric Boundary Layer) ABL that conforms to established standards. This study focuses on achieving such a simulation in the (Boundary Layer Wind tunnel) BLWT at the University of Bristol.

To ensure the ABL's fidelity, initial efforts were directed at characterising the wind tunnel under two conditions: with an empty test section and with Counihan method [1] components installed. These components, including roughness elements and vortex generators, are designed to replicate urban turbulence conditions and align with methodologies used in similar studies [2, 3].

While previous works [4, 5] have analysed flow properties in idealised scaled city models using wind tunnel measurements, a notable gap exists in incorporating terrain topology into experimental setups. Terrain variations significantly influence urban ABL development, yet many studies overlook this factor. Addressing this gap, our work integrates both building canopy effects and topographical features into the experimental framework, enabling a more comprehensive analysis of urban flow dynamics.

This study will focus on generating a validated ABL, characterising its behaviour over a scaled urban model, and investigating the combined impact of terrain and building geometry. These efforts aim to enhance the understanding of urban aerodynamic phenomena and provide a robust foundation for future computational and experimental research. Additionally, the data generated in this study can be leveraged by computational partners to initiate and validate their (Computational Fluid Dynamics) CFD simulations, ensuring greater accuracy and reliability in modelling complex urban environments.

## 2. Atmospheric boundary layer generation

### 2.1. Experimental set-up

The BLWT at the University of Bristol spans 30 *m* and features nine axial fans with a total power of 240 *kW*, offering adjustable operational modes to achieve flow velocities between 0.5 *m/s* and 35 *m/s* with low turbulence. The test section, measuring 2 *m* wide, 1 *m* high, and 18 *m* long, naturally develops a boundary layer (BL) exceeding 200 *mm* thickness ( $Re_x \sim 9.5 \times 10^6$ ) [6].

## EXPERIMENTAL DATABASES



For the experimental setup simulating the ABL, components were designed based on [1, 7, 8], detailed in Figure 1, with  $H = 900 \text{ mm}$  being the height of vortex generators, with a spacing of  $0.6H$ , and the height of the castellated barrier is  $200 \text{ mm}$ . The Lego blocks, that represent the roughness elements in the Counihan's method [1], have a height of  $60 \text{ mm}$ , and they were in a staggered pattern with a spacing of  $140 \text{ mm}$ .

The instrumentation included Dantec 55P15 single-wire probes for smooth wall configurations, and 55P51 crosswire hot-wire probes for ABL configurations, that were mounted on the linear traverse system SMC-LEFS32 of  $1000 \text{ mm}$  stroke and a  $0.01 \text{ mm}$  precision (along  $y$ -direction). The data acquisition was controlled using Labview. The calibration of the probes was conducted using a 54H10 calibrator and StreamWare Pro v6.00 software. Hot-wire measurements were executed using a Dantec Streamline ProSystem equipped with a CTA91C10 module, interfaced with a National Instruments PXIe-4499 module housed in a PXIe-1082Q chassis for data acquisition. Data was sampled at a rate of  $2^{16} \text{ Hz}$ , with sampling times initially estimated using [9], then optimised based on several tests to be  $100 \text{ s}$  per measurement point, with the measurements taken at  $700 \text{ mm}$  distance from the last row of roughness elements ( $x = 700 \text{ mm}$ ).

In addition to ABL generation characterisation, the airflow properties in the empty tunnel were evaluated at different speeds  $10, 15$  and  $20 \text{ m/s}$ , the homogeneity of the flow spanwise ( $z$ -direction) was validated for both mean velocity measurements and turbulence intensity.

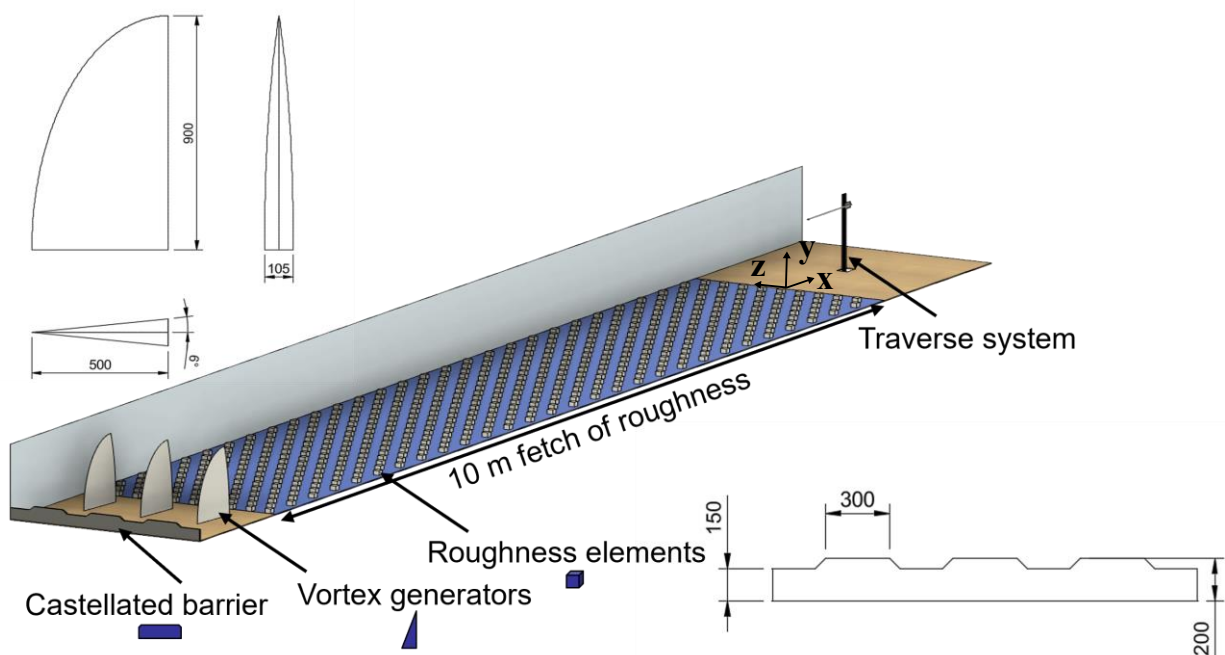


Figure 1: Counihan method for generating ABL components.

## 2.2. Results and discussion

To investigate the suitability of the generated BL as a representation of ABL in urban flow, Figure 2 (a) illustrates the power law, i.e.  $\frac{U}{U_{ref}} = \left(\frac{y-d}{y_{ref}-d}\right)^\alpha$  with  $U$ ,  $\alpha$ ,  $d$ ,  $U_{ref}$ , and  $y_{ref}$  being the mean velocity in  $x$ -direction, the power law exponent, zero-plane displacement, mean velocity and height at a reference point, respectively. The value of  $\alpha$  represents how rough is the canopy of the ABL, and the value of  $d$  represents the origin of the measurements, and the ESDU [10] provides the acceptable ranges for these values in the case of urban flows.

By fitting the data to the power law, the power-law exponent reached a value of  $= 0.32$ ; that is in the range of urban flows according to ESDU [10], and the zero-displacement height was found to be about  $d = 9.32 \text{ mm}$ . The turbulence intensity  $I_u = \sqrt{u'^2}/U$ , in percentage, with  $u'$  the fluctuating velocity component in the  $x$ -direction, shown in Figure 2 (b), is within the 30% confidence interval of the ESDU [10] up to a height of  $300 \text{ m}$  in full-scale, which is the available data according to ESDU [10].

To further investigate the ABL characteristics, the power spectral of longitudinal velocity fluctuations  $P_{uu}(f)$  at an arbitrary chosen point  $y = 255 \text{ mm}$  within the ABL, was calculated; it represents how the energy of velocity variations in the flow is distributed across different frequencies  $f$ , providing insight into the turbulent energy at various scales. As shown in Figure 2 (d),  $P_{uu}(f)$  demonstrates a clear inertial subrange, indicated by the  $-5/3$  slope in the log-log scale. This behavior is consistent with Kolmogorov's theory of turbulence [11], which predicts a universal energy cascade in fully developed turbulence providing validation for the flow's fidelity and reinforcing the suitability of the experimental setup for studying urban boundary layer characteristics. The aerodynamic surface roughness length  $y_0$  was determined by fitting the experimental data to the logarithmic velocity profile law:

$$U = \frac{u_\tau}{k} \ln\left(\frac{y-d}{y_0}\right),$$

where  $u_\tau$  is the friction velocity, and  $k$  is the von Kármán constant, taken as 0.4. The friction velocity  $u_\tau$  was calculated using the wall similarity method of Clauser [16], resulting in a surface roughness length of  $y_0 = 4.17 \text{ mm}$ .

Another key characteristic in evaluating urban ABLs is ensuring the integral length scales are within acceptable norms. Here, the criterion is based on Walshe's theory [12]. The integral length scales of turbulence  $L_{ux}$  were calculated using autocorrelation functions under the assumption of Taylor's hypothesis  $L_{ux} = U \int R_{uu}(t) dt$ , with  $R_{uu}$  the longitudinal autocorrelation coefficient. Figure 2 (c) demonstrates that the computed integral

# EXPERIMENTAL DATABASES



length scales are within the 30% limits of Walshe's [12] theoretical range:  $L_{ux} = 101 (y/10)^\alpha$ , up to a height of 400 m in full scale, which is the applicable range height available for this type of data.

To utilise the generated urban ABL flows over city models, an appropriate scaling must be established. Using Cook's method [13], the scale  $S$  is determined by:

$$S = \frac{91.3 (y - d)^{0.491}}{L_{ux}^{1.403} y_0^{0.088}}$$

In this context, the integral length scale  $L_{ux}$  was estimated by fitting the measured data to Cook's [13] design curve and calculating  $L_{ux}$  using the relation  $f \frac{L_{ux}}{U} = 1$  with  $f$  the lowest measured frequency. Based on this deterministic approach, the scale for the urban flow was determined to be 1: 800.

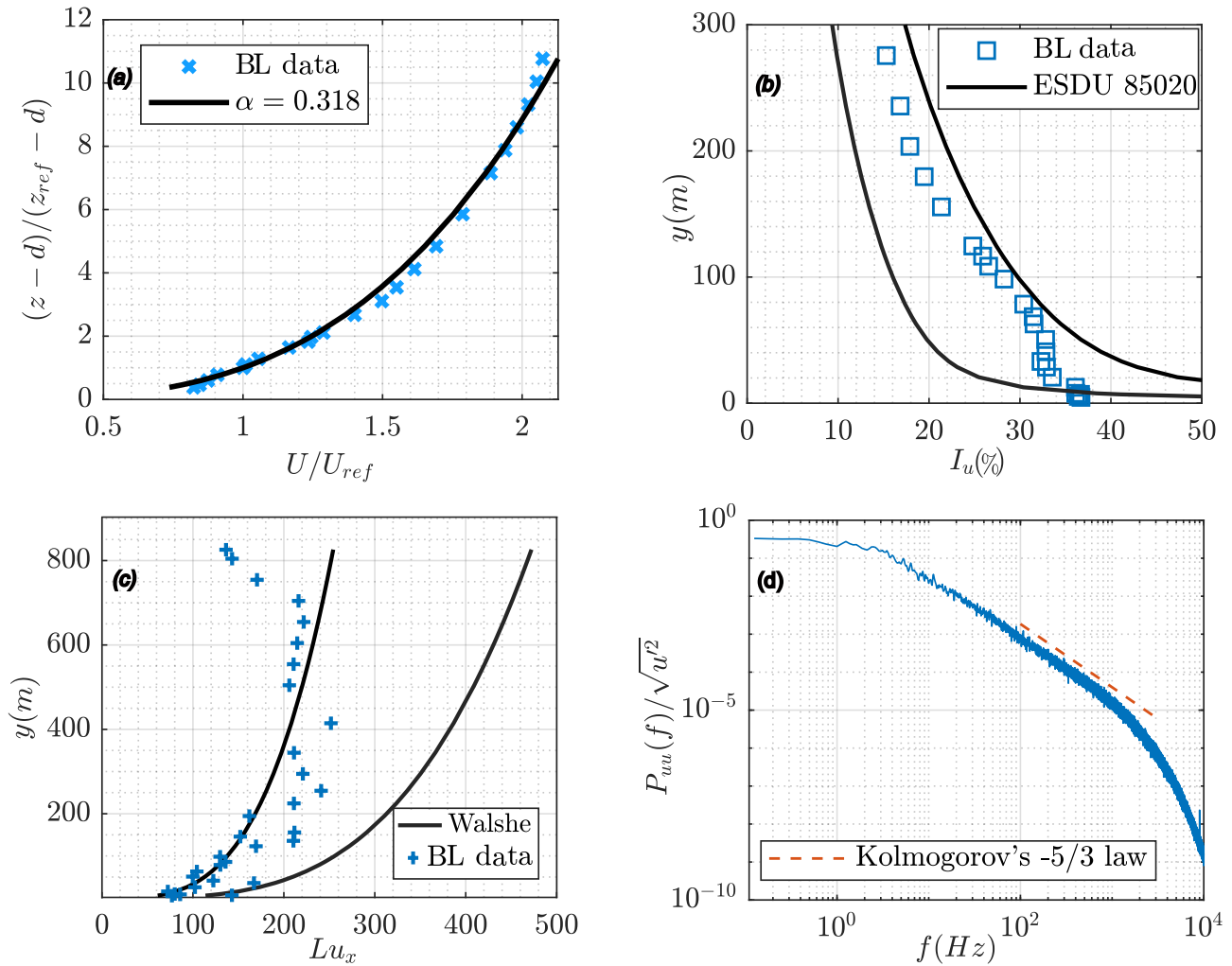


Figure 2: (a) Mean velocity profile compared to the power law with  $\alpha=0.318$ , (b) Turbulence intensity compared to  $\pm 30\%$  ESDU 85020 confidence interval ( $y$  in full scale, with scale 1:800), (c) Integral length scale  $L_{ux}$  in full scale compared to Walshe theory, and (d) Power spectral density of at  $y=255$  mm and  $x=0$  mm.



## 3. Bristol city wind tunnel model

### 3.1. Experimental set-up

Velocity measurements were conducted over a scaled model of Bristol city, focusing on a central area covering  $1052\text{ m} \times 2040\text{ m}$ , shown in Figure 3. The model was scaled down using the previously determined scale of 1:800, and its design was based on Ordnance Survey data [14], incorporating both idealised flat building structures and terrain topography. Notably, the terrain height variations in this area were significant compared to building heights, with the highest terrain point reaching up to  $75\text{ m}$ . Key high-rise buildings within the selected area are listed in Table 1.

Table 1: Key high-rise buildings within the selected area.

Building	Full scale (m)	Scale 1:800 (mm)
Bristol Royal Infirmary	38	47.5
Queen’s building	41	51.25
New Bridewell Tower	49	61.25
Number one Bristol	59	73.75
St.Nicholas Church	60	75
Premier Inn Bristol City Centre	60	75
Fusion Tower	63	78.75
Beacon Tower	64	80
Eclipse	65	81.25
Castlemead	80	100
Castle Park view	98	122.5

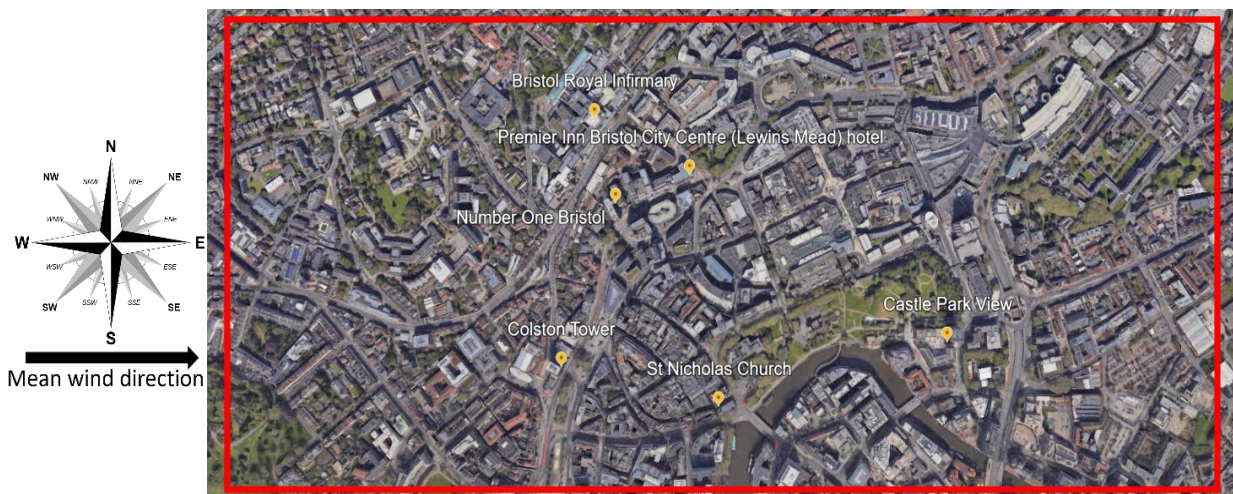


Figure 3: Bristol city area of interest.

## EXPERIMENTAL DATABASES



For manufacturing the city model, the in-house CNC machine Denford600, shown in Figure 4, was chosen over 3D-printing due to its lower cost, shorter lead time, ease of installation, and the lightweight properties of the extruded polystyrene XPS X 500 SL used. Another critical consideration was aligning the model with Bristol's prevailing wind direction, which is predominantly from the west, Figure 5. To address the abrupt step between the wind tunnel floor and the model, a smoothing ramp was designed and installed to ensure a smooth BL transition and minimise sudden pressure gradients. The ramp, 800 mm in length, shown in Figure 6, was constructed using a spline-based design, with control points ensuring zero gradient at both ends.



Figure 4: Denford 6600 Pro CNC machine.

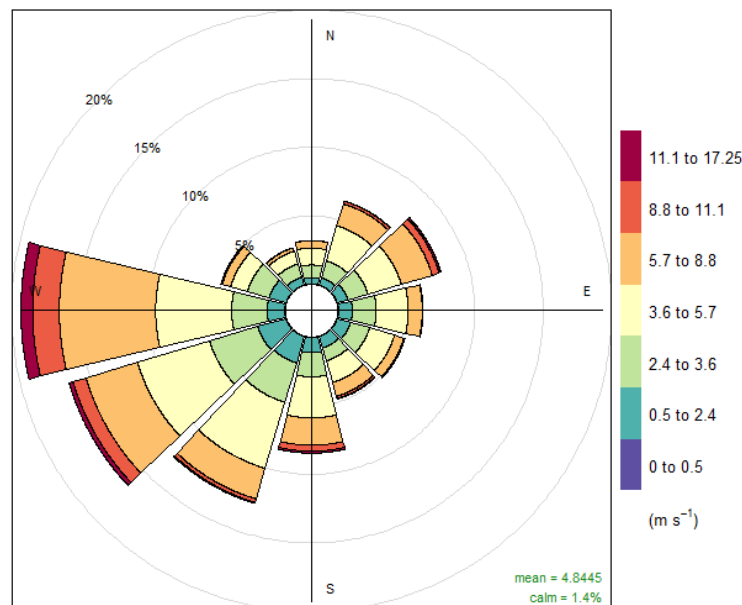


Figure 5: Bristol city wind rose using frequency of counts by wind direction (%) with the sensor base at Bristol airport [17].

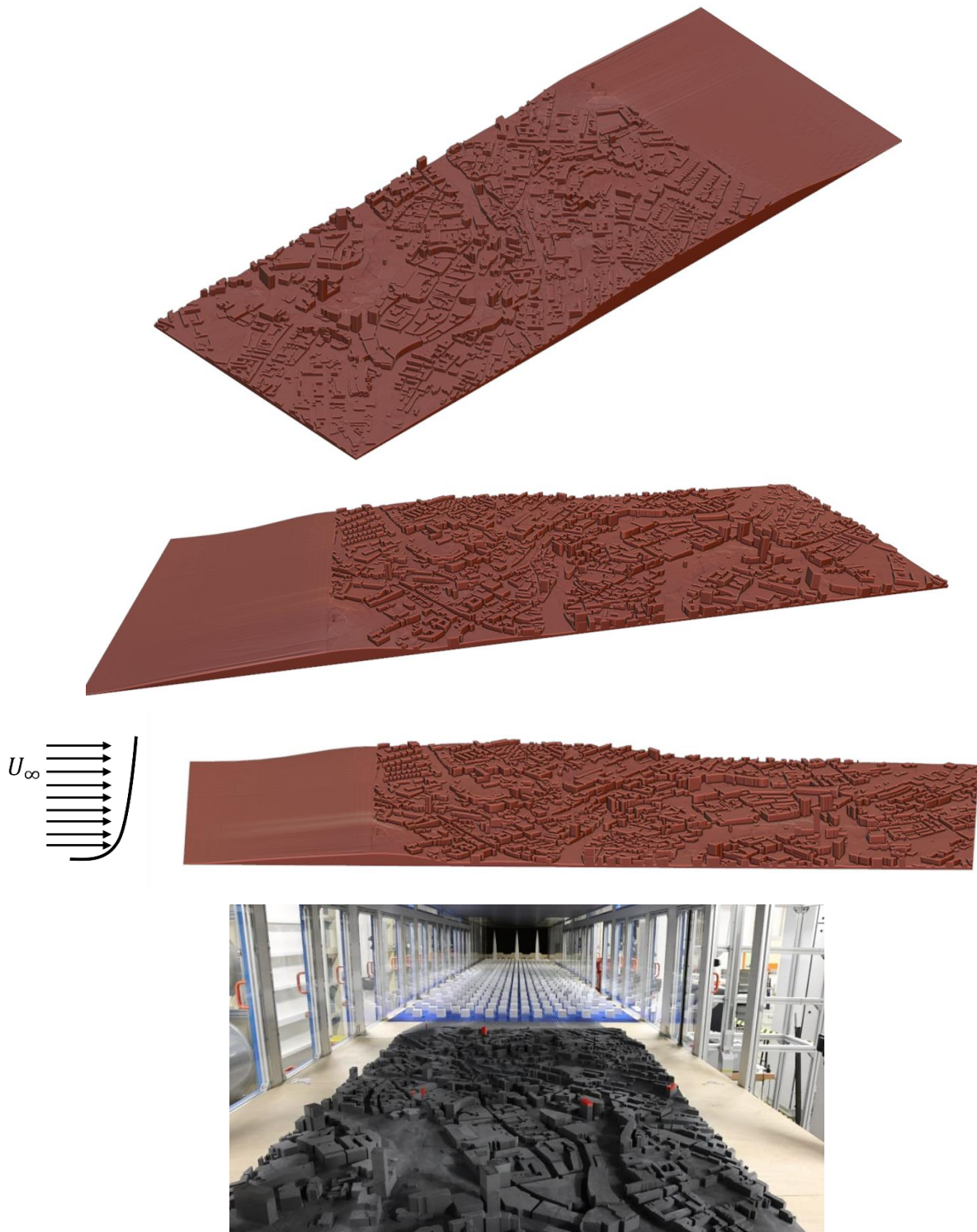


Figure 6: Bristol city model with smoothing ramp and its installation inside the BLWT.

Velocity measurements were taken at various locations on the model, as shown in the Figure 7, using hot-wire anemometry. All the measurements were done using a wind tunnel speed of 10 m/s. Sampling times were set to 100 s per point, and vertical velocity profiles were measured at the ramp entrance, the city's

entrance (ramp exit), and multiple locations throughout the city. These measurements aimed to analyse the effects of building canopy and terrain topography on flow development across the city. All the measurement heights  $y$  were measured by taking the direct perpendicular location as an origin.

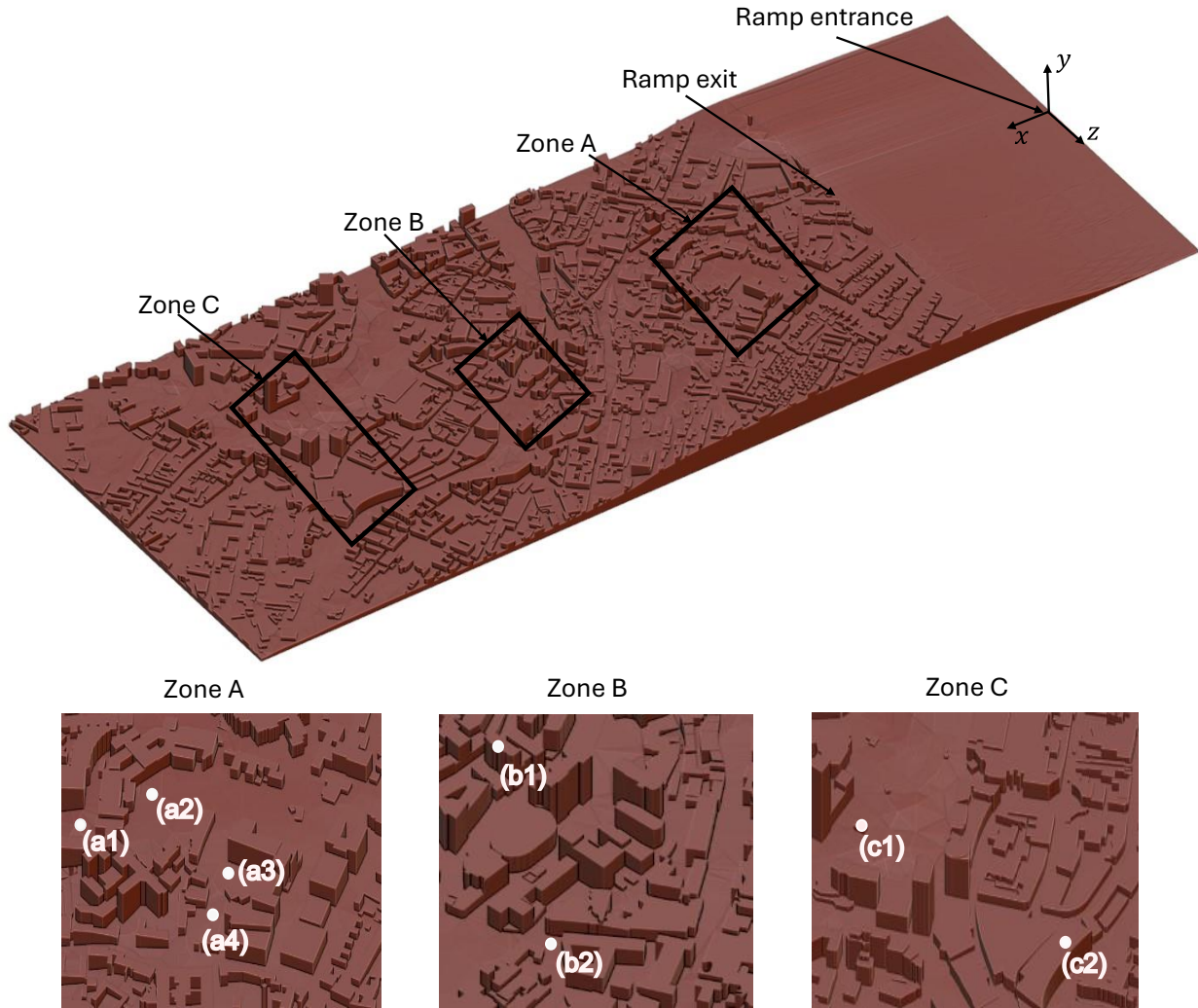


Figure 7: Measurements locations on the ramp and through the city model.

## 3.2. Results and discussion

### 3.2.1. City inflow conditions: smoothing ramp analysis

The results in Figure 8 are comparing the mean velocity profiles for two cases: with and without the city model. The comparison reveals that the profiles align closely in the outer region, with the influence of the city diminishing at a height of  $y = 10 \text{ cm}$ , corresponding to the highest point at the entrance of the city model.

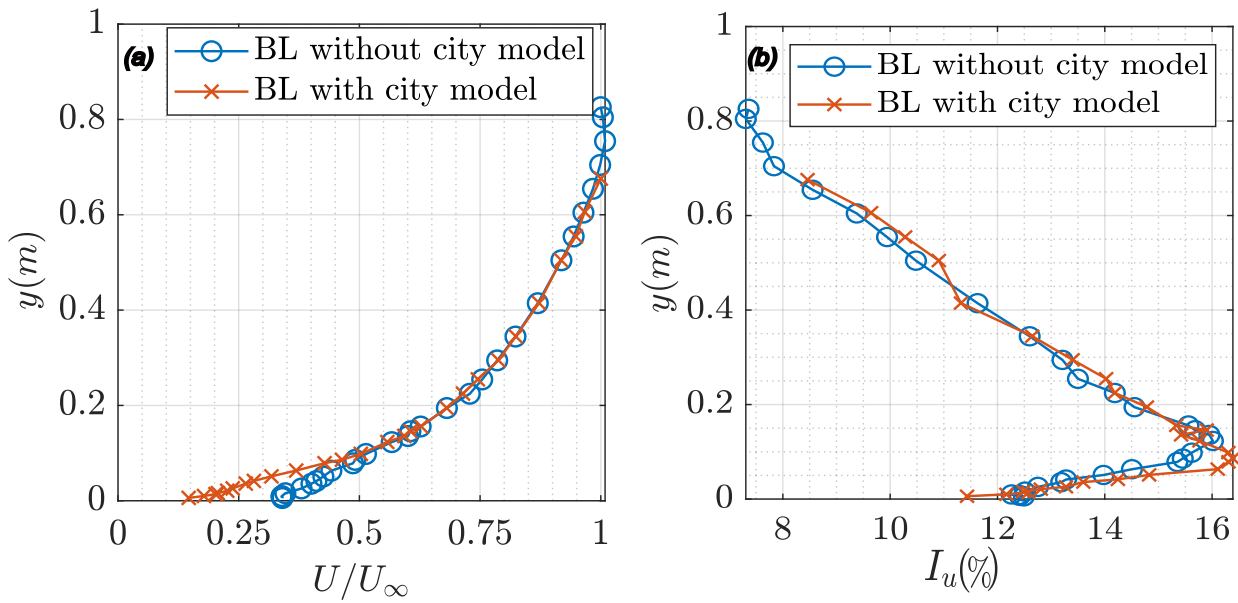


Figure 8: Effect of city model on incoming flow BL (a) mean velocity, and (b) turbulence intensity at  $x=0\text{mm}$  and  $z=0\text{mm}$ .

To ensure that the incoming ABL is spanwise homogeneous, tests were conducted at the entrance of the ramp (i.e.,  $x = 0$ ) at three different spanwise locations:  $z = 0\text{ mm}$ ,  $z = -225\text{ mm}$ , and  $z = +225\text{ mm}$ . Figure 9 illustrates the mean velocity and turbulence intensities measured at these locations. The deviation in mean velocity across the spanwise positions is within the acceptable range as specified in [15]. For turbulence intensity, a deviation of approximately 2% was observed between the center position and the other spanwise locations. This discrepancy may be attributed to interactions caused by spanwise vortices.

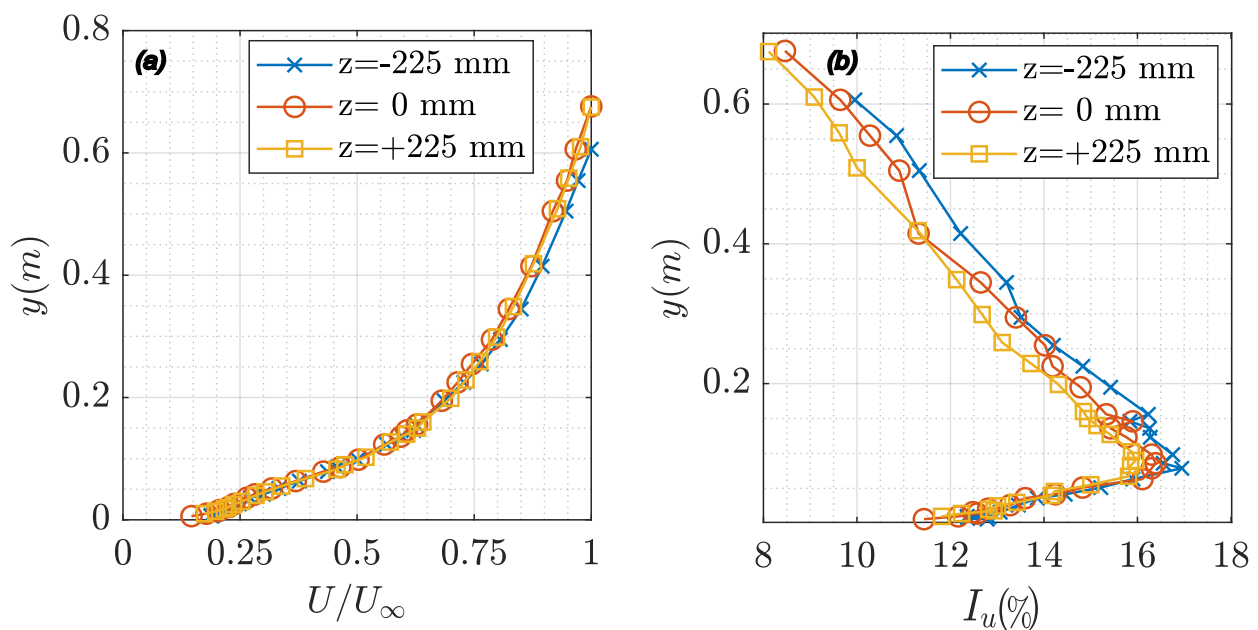


Figure 9: Spanwise homogeneity analysis of incoming flow BL of (a) mean velocity, and (b) turbulence intensity at  $x=0\text{ mm}$  and  $z=0\text{ mm}$ .

## EXPERIMENTAL DATABASES



At the exit of the ramp, which corresponds to the entrance of the city  $x = 800 \text{ mm}$ , measurements were taken at the centreline  $z = 0 \text{ mm}$ , to characterise the flow immediately entering the city after the ramp smoothing. Figure 10 presents both the mean velocity and turbulence intensity at this location. This data will be valuable for future Computational Fluid Dynamics (CFD) analysis, serving as a reference for cross-evaluation later in the project.

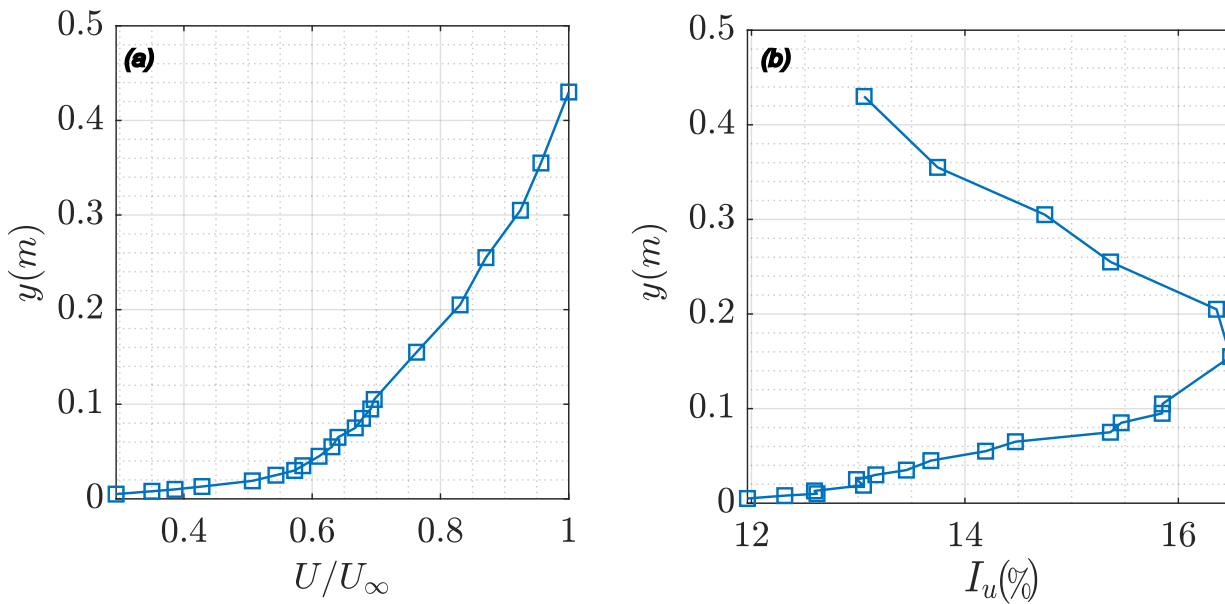


Figure 10: Measurements at ramp exit of (a) mean velocity, and (b) turbulence intensity at  $x=800 \text{ mm}$  and  $z=0 \text{ mm}$ .

### 3.2.2. Flow throughout the city model

To analyse the flow development through the city, measurements were conducted in areas (a), (b), and (c), as indicated in Figure 7. Various locations within these areas were assessed, and the normalised mean velocity  $U$  and turbulence intensity  $I_u$  are presented in Figures 11 to 18. The initial data, collected from locations featuring both canopy and topographical changes, indicate that both factors influence the development of the ABL. These measurements provide insight into the flow dynamics and turbulence distribution over the urban model. Further investigations will be conducted using Particle Image Velocimetry (PIV) to capture detailed flow characteristics in the key areas where significant changes occur.

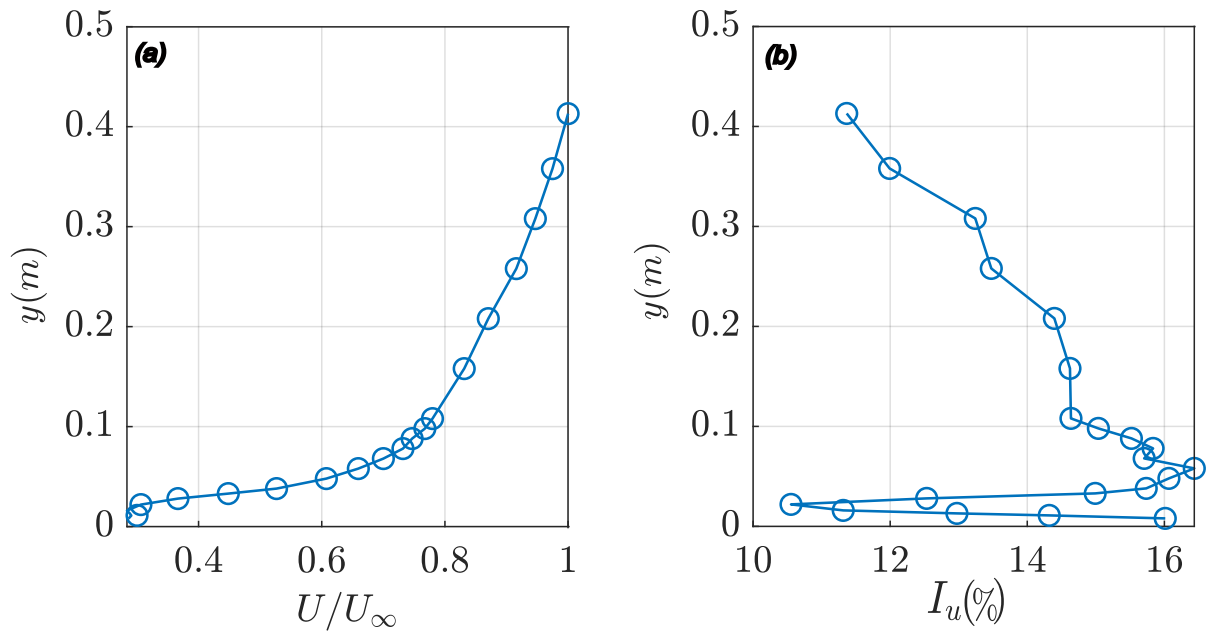


Figure 11: Measurements at location a1 of (a) mean velocity, and (b) turbulence intensity.

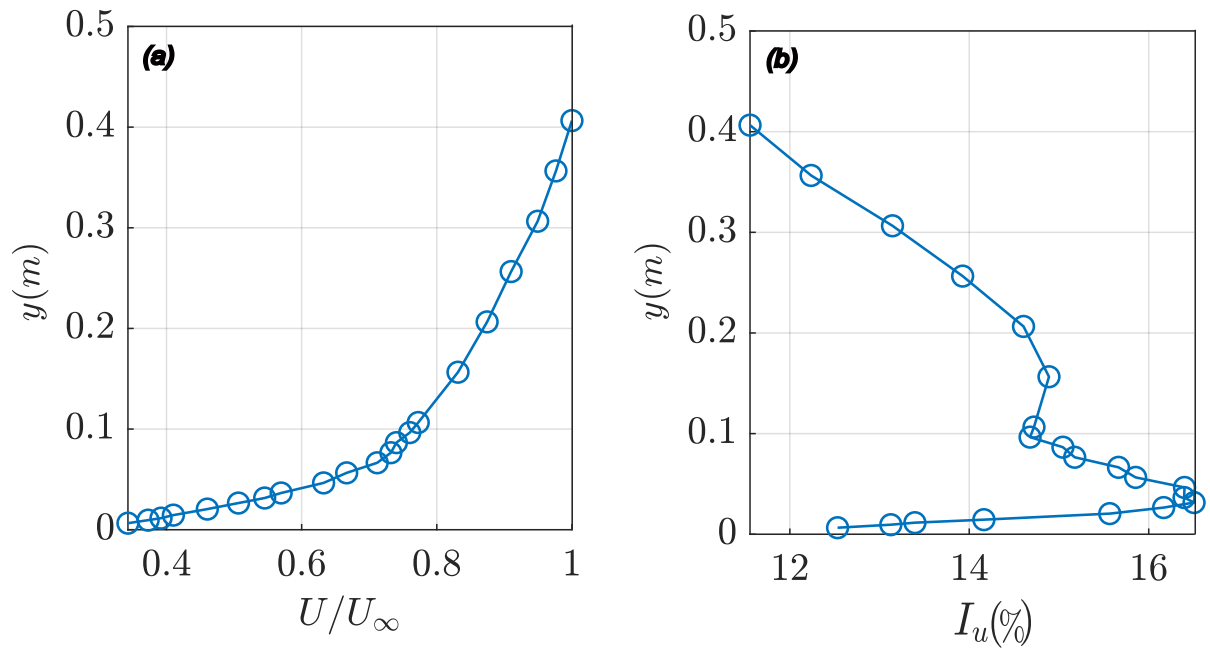


Figure 12: Measurements at location a2 of (a) mean velocity, and (b) turbulence intensity.

# EXPERIMENTAL DATABASES

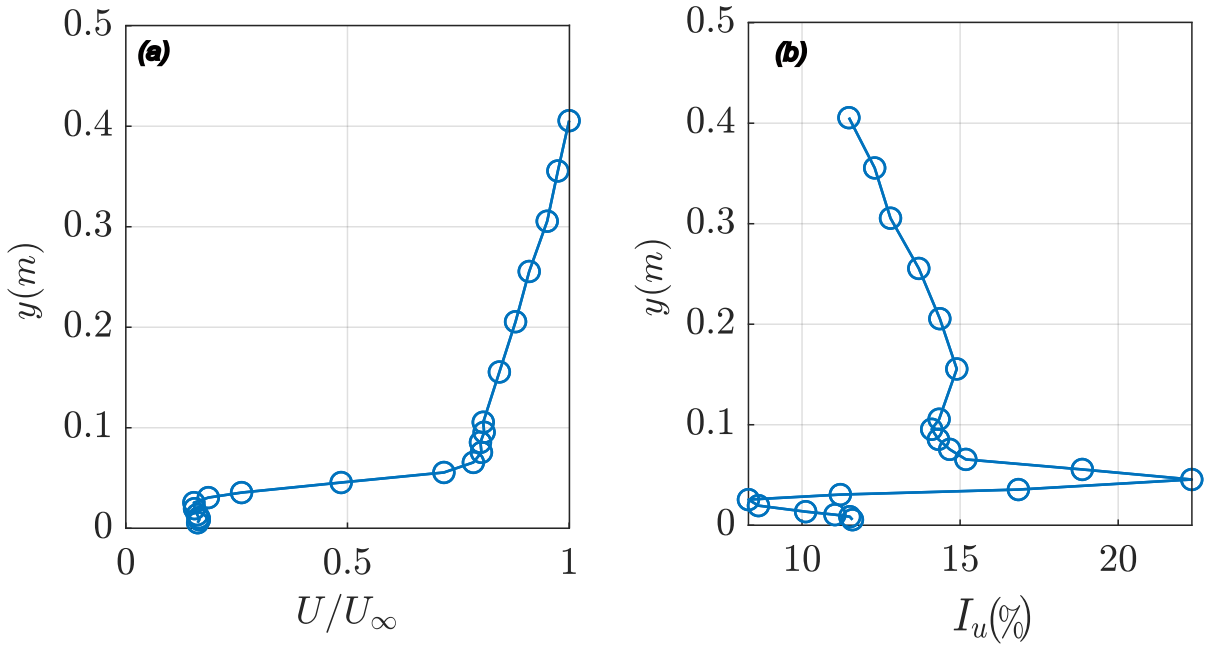


Figure 13: Measurements at location a3 of (a) mean velocity, and (b) turbulence intensity.

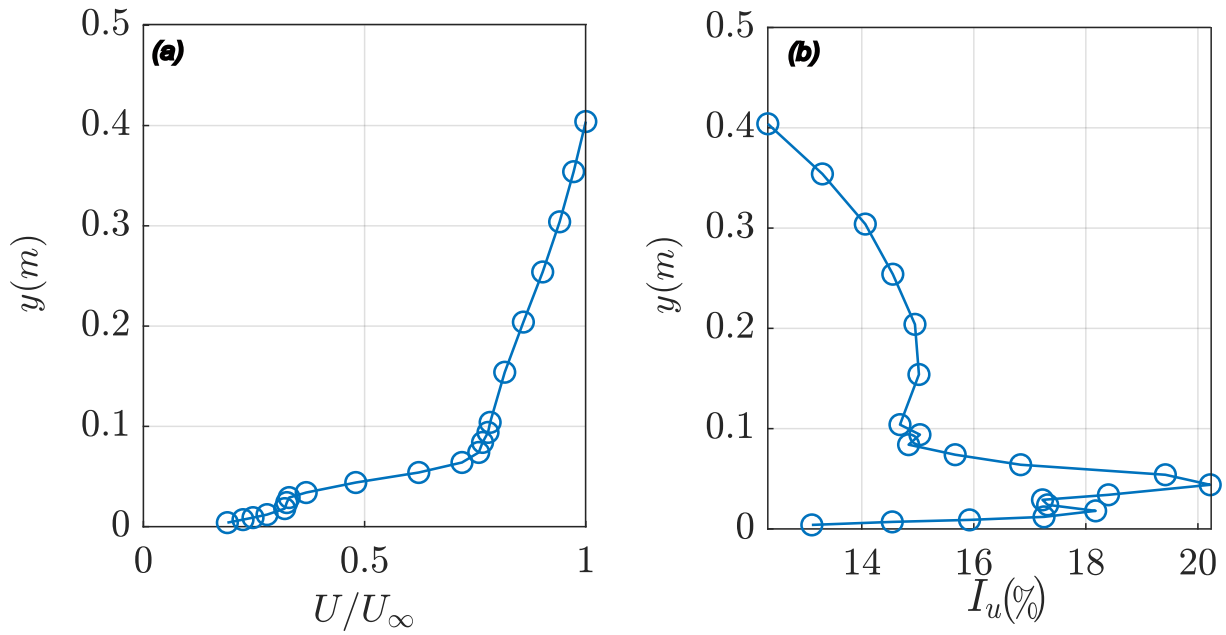


Figure 14: Measurements at location a4 of (a) mean velocity, and (b) turbulence intensity.



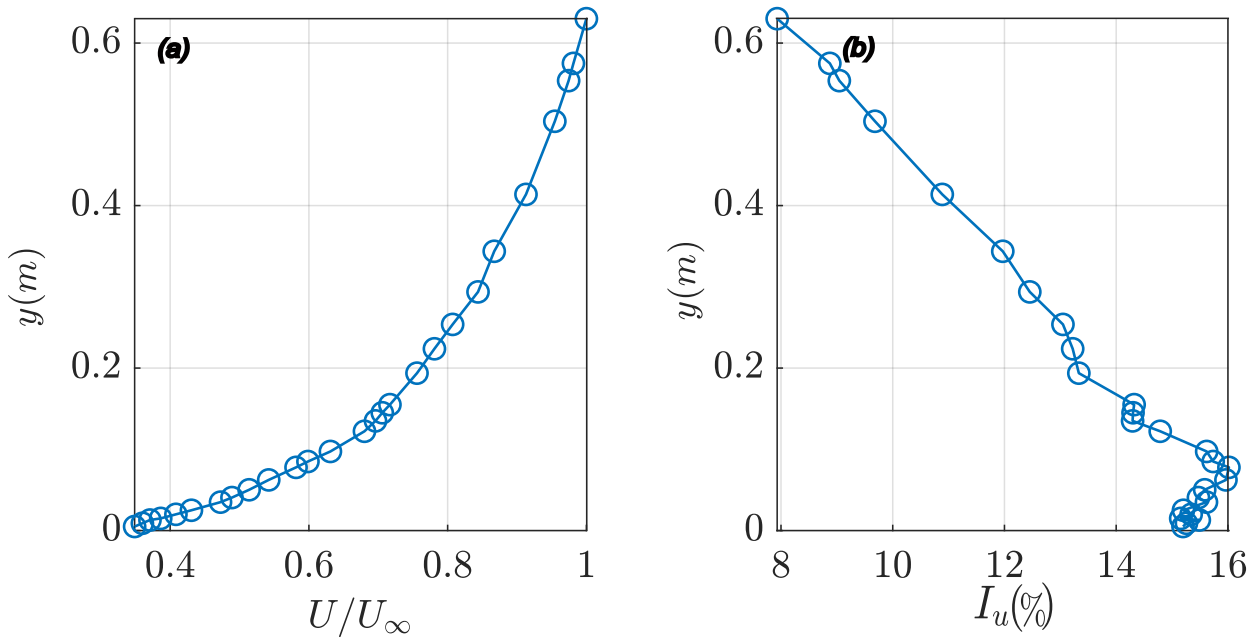


Figure 15: Measurements at location b1 of (a) mean velocity, and (b) turbulence intensity.

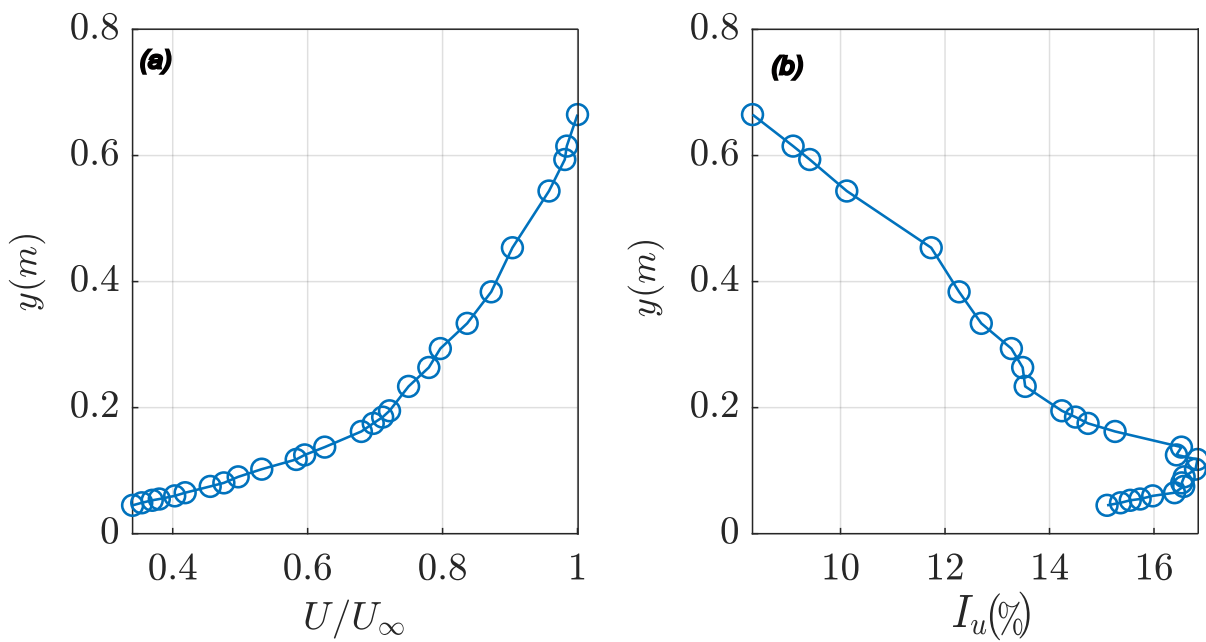


Figure 16: Measurements at location b2 of (a) mean velocity, and (b) turbulence intensity.

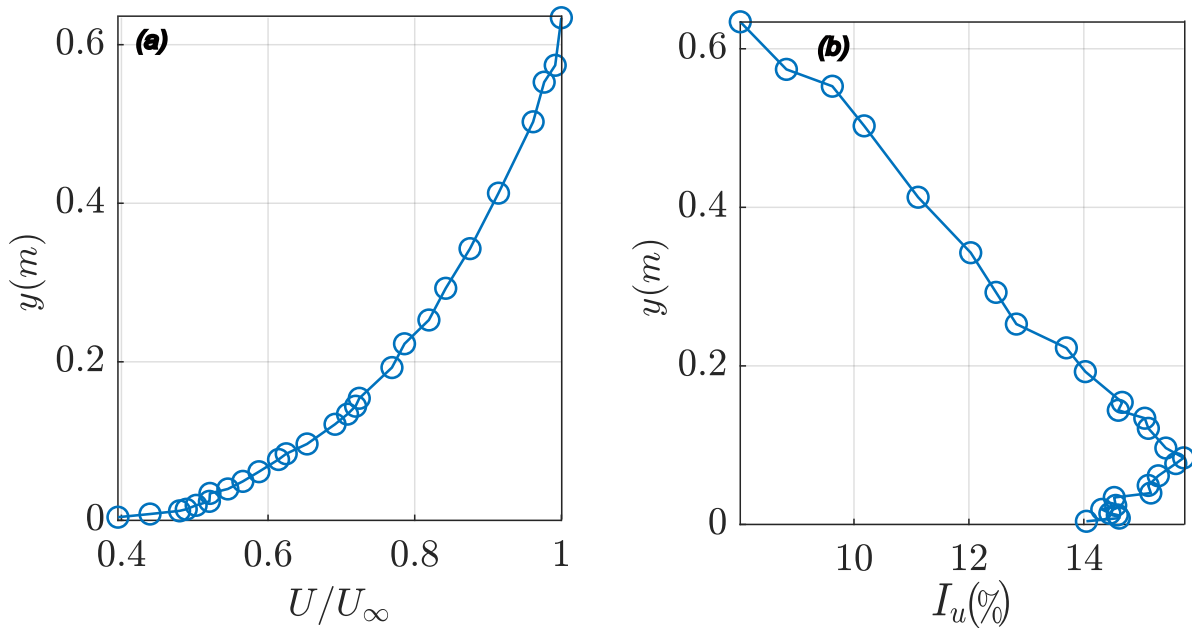


Figure 17: Measurements at location c1 of (a) mean velocity, and (b) turbulence intensity.

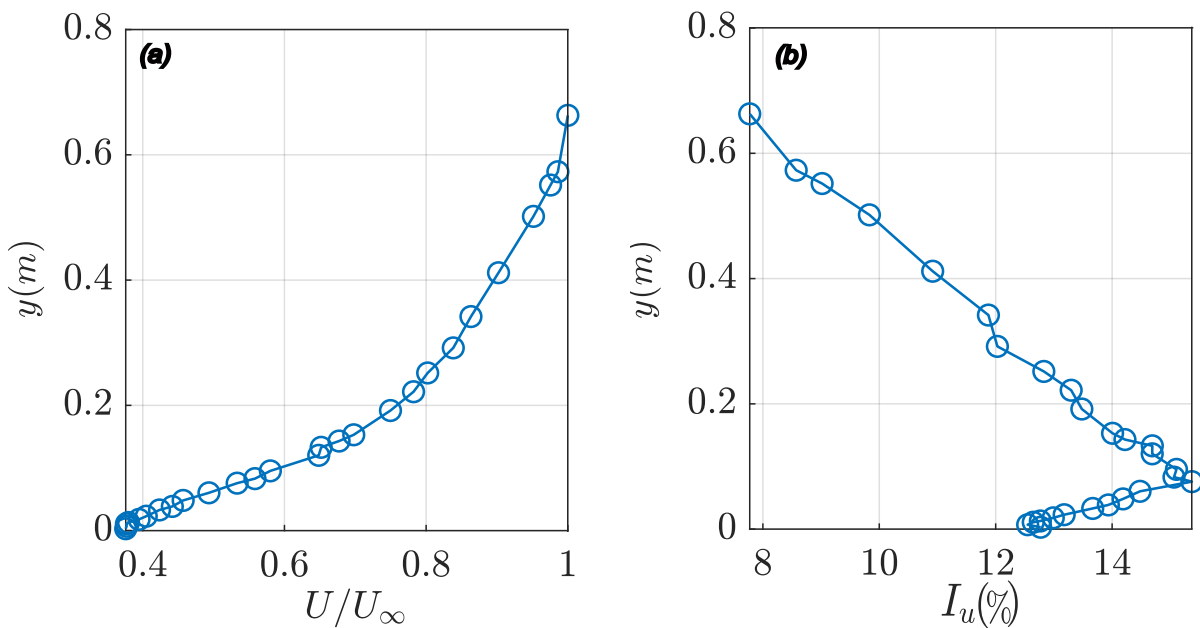


Figure 18: Measurements at location c2 of (a) mean velocity, and (b) turbulence intensity.

To examine the flow dynamics in the region near a building, measurements were conducted at location a2, positioned behind Queen’s building, Figure 7. The power spectral of longitudinal velocity fluctuations  $P_{uu}(f)$  was plotted at various heights  $y$  within the range of 0 to 500 mm, as indicated by an arrow on Figure 19. The results demonstrate a clear adherence to Kolmogorov’s  $-5/3$  power law, highlighting the characteristic

energy cascade within the inertial subrange of turbulent flow. These findings confirm the presence of well-developed turbulence and provide insights into the dynamics influenced by the building geometry.

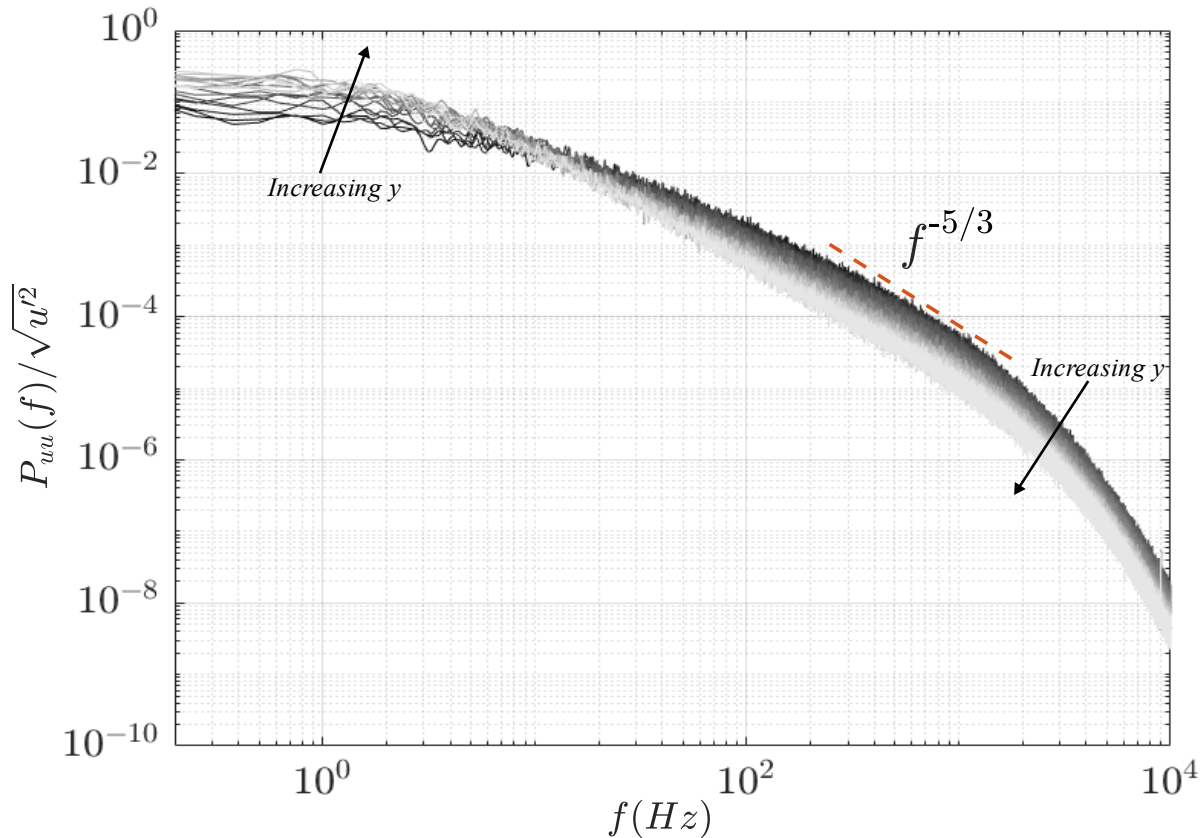


Figure 19: Power spectral density of measurements at location (a2) over  $0 < y < 500$  mm. The color of the line plots corresponds to the wall-normal distance, with dark gray indicating  $y$ -values near the wall and light gray representing  $y$ -values farther from the wall.

## 4. Conclusions and future work

In conclusion, the established ABL conforms to the ESDU and Walshe standards, making it suitable for conducting urban flow experiments. While the current measurements around the city model are preliminary, they provide valuable insights into the flow characteristics within the urban environment. Future work will leverage a newly installed 3D traverse system within the wind tunnel to enable coupled hot-wire measurements and Flame Ionisation Detector (FID) analysis, facilitating detailed velocity and concentration distribution mapping. Additionally, Particle Image Velocimetry PIV will be employed to investigate areas of interest more closely, offering visualisations of flow development along the city model and enhancing the understanding of urban aerodynamic phenomena.

# EXPERIMENTAL DATABASES



## Acknowledgements

This project has received funding from the European Union's Horizon Europe research and innovation program under the MODELAIR project grant agreement No.101072559.

## References

- [1] Counihan, J. (1969). An improved method of simulating an atmospheric boundary layer in a wind tunnel. *Atmospheric Environment* (1967), 3(2), 197–214. [https://doi.org/10.1016/0004-6981\(69\)90008\\_0](https://doi.org/10.1016/0004-6981(69)90008_0)
- [2] Kozmar, H. (2011). Characteristics of natural wind simulations in the TUM boundary layer wind tunnel. *Theoretical and Applied Climatology*, 106(1-2), 95–104. <https://doi.org/10.1007/s00704-011-0417-9>
- [3] Cook, N. J. (1978b). Wind-tunnel simulation of the adiabatic atmospheric boundary layer by roughness, barrier and mixing-device methods. *Journal of Wind Engineering and Industrial Aerodynamics*, 3(2-3), 157–176. [https://doi.org/10.1016/0167-6105\(78\)90007-7](https://doi.org/10.1016/0167-6105(78)90007-7)
- [4] Castro, I. P., Xie, Z.-T., Fuka, V., Robins, A. G., Carpentieri, M., Hayden, P., Hertwig, D., & Coceal, O. (2016). Measurements and Computations of Flow in an Urban Street System. *Boundary-Layer Meteorology*, 162(2), 207–230. <https://doi.org/10.1007/s10546-016-0200-7>
- [5] Hertwig, D., Grimmond, S., Kotthaus, S., Vanderwel, C., Gough, H., Haeffelin, M., & Robins, A. (2021). Variability of physical meteorology in urban areas at different scales: implications for air quality. *Faraday Discussions*, 226, 149–172. <https://doi.org/10.1039/d0fd00098a>
- [6] University of Bristol. (2024). Hele-Shaw Boundary Layer Wind Tunnel, Boundary Layer WT. <https://www.bristol.ac.uk/aerodynamics-research/facilities/boundary-layer> (Accessed: 31 July 2024).
- [7] Hohman, T. C., Buren, T. V., Martinelli, L., & Smits, A. J. (2015). Generating an artificially thickened boundary layer to simulate the neutral atmospheric boundary layer. *Journal of Wind Engineering and Industrial Aerodynamics*, 145, 1–16. <https://doi.org/10.1016/j.jweia.2015.05.012>
- [8] Gartshore, I. S., & De Croos, K. A. (1977). Roughness Element Geometry Required for Wind Tunnel Simulations of the Atmospheric Wind. *Journal of Fluids Engineering*, 99(3), 480–485. <https://doi.org/10.1115/1.3448821>
- [9] Hauptman, Z. (2010). Characterization of a low-speed boundary layer wind tunnel. *Master's Theses and Capstones*, 549.
- [10] Engineering Sciences Data Unit. (1985). Characteristics of atmospheric turbulence near the ground, Data Item 85020. ESDU International Ltd, London.
- [11] Kolmogorov, A. N. (1941). The Local Structure of Turbulence in Incompressible Viscous Fluid for Very Large Reynolds' Numbers. *Proceedings of the USSR Academy of Sciences*, 30, 301–305.
- [12] Walshe, D. E. J. (1972). Wind-excited oscillations of structures. National Physical Laboratory, 61–67.

## EXPERIMENTAL DATABASES



- [13]Cook, N. J. (1978a). Determination of the model scale factor in wind-tunnel simulations of the adiabatic atmospheric boundary layer. *Journal of Wind Engineering and Industrial Aerodynamics*, 2(4), 311–321. [https://doi.org/10.1016/0167-6105\(78\)90016-8](https://doi.org/10.1016/0167-6105(78)90016-8)
- [14]Department for Environment Food & Rural Affairs (DEFRA). (2024). *Defra Data Services Platform*. Environment.data.gov.uk. <https://environment.data.gov.uk/survey> (Accessed: 31 July 2024).
- [15]Balendra, T., Shah, D. A., Tey, K. L., & Kong, S. K. (2002). Evaluation of flow characteristics in the NUS-HDB Wind Tunnel. *Journal of Wind Engineering and Industrial Aerodynamics*, 90(6), 675–688. [https://doi.org/10.1016/s0167-6105\(01\)00223-9](https://doi.org/10.1016/s0167-6105(01)00223-9)
- [16]Clauser, F. H. (1954). Turbulent boundary layers in adverse pressure gradients. *Journal of the Aeronautical Sciences*, 21(2), 91–108.
- [17]Carslaw, D. C. and K. Ropkins, (2012). Openair: an R package for air quality data analysis. *Environmental Modelling & Software*, 27-28, 52-61.